Altered directed functional connectivity of the right amygdala in depression: high-density EEG study

Alena Damborská[1,2 a *], Maria Rubega [1a], Eliška Honzírková [2], Richard Barteček [2], Jana Hořínková [2], Sylvie Fedorová [2], Šimon Ondruš [2], Christoph M. Michel [1,3]

[1]Department of Basic Neurosciences, University of Geneva, Campus Biotech, Geneva, Switzerland
[2]Department of Psychiatry, Faculty of Medicine, Masaryk University and University Hospital Brno, Brno, Czech Republic
[3]Lemanic Biomedical Imaging Centre (CIBM), Lausanne and Geneva, Switzerland

[a] these authors contributed equally to this work

*** Correspondence:**
Alena Damborská
Alena.Damborska@unige.ch

Keywords: Directed functional connectivity, Electrical source imaging, High-density EEG, Resting-state, Major depressive disorder, Bipolar disorder, Deep-brain stimulation targets.

Abstract

Background: The cortico-striatal-pallidal-thalamic and limbic circuits are suggested to play a crucial role in the pathophysiology of depression. Stimulation of deep brain targets might improve symptoms in treatment-resistant depression. Better understanding of connectivity properties of deep brain structures potentially implicated in DBS treatment is needed.

Methods: Using high-density EEG, we explored the directed functional connectivity at rest in 25 healthy subjects and 26 patients with moderate to severe depression within the bipolar affective disorder, depressive episode, and periodic depressive disorder. We computed the Partial Directed Coherence on the source EEG signals arising from the amygdala, anterior cingulate, putamen, pallidum, caudate, and thalamus. The global efficiency for the whole brain and the local efficiency, clustering coefficient, outflow, and strength for the selected structures were calculated.
Results: In the right amygdala, all the network metrics were significantly higher ($p<0.001$) in patients than in controls. The global efficiency was significantly higher ($p<0.05$) in patients than in controls, showed no correlation with status of depression, but decreased with increasing medication intake ($R^2 = 0.59$ and $p_{value} = 1.52\text{e} - 05$).

Conclusion: The amygdala seems to play an important role in neurobiology of depression and as such could be considered as a potential future target for DBS in treating treatment-resistant depression.

1 Introduction

Affective disorders are among the most common and most serious psychiatric disorders (1). Crucial role of the cortico-striatal-pallidal-thalamic and limbic circuits in the pathophysiology of depression was repeatedly reported (2) (3) (4). Magnetic resonance imaging, functional magnetic resonance imaging (fMRI), magnetoencephalographic, and electroencephalographic (EEG) studies have confirmed that depressive patients show structural impairments and disbalances in a coordinated activity of several brain regions considered to be important for a) emotions, i.e. amygdala, subgenual

anterior cingulate, caudate, putamen and pallidum (5) (3) (6) (7) (8) (9) (10) (11) (12); b) self-referential processes, i.e. medial prefrontal cortex, precuneus, and posterior cingulate cortex (13) (14); c) memory, i.e. hippocampus, parahippocampal cortex (15); d) visual processing, i.e. fusiform gyrus, lingual gyrus, and lateral temporal cortex (16); and e) attention, i.e. dorsolateral prefrontal cortex, anterior cingulate cortex (ACC), thalamus, and insula (17) (10) (11) (12). Moreover, post-mortem morphometric measurements revealed smaller volumes of the hypothalamus, pallidum, putamen and thalamus in patients with affective disorders (18).

Many depressive patients fail to respond to pharmacological therapy resulting in 1 – 3% prevalence of treatment-resistant depression (TRD) (19). One of the newest therapeutic alternatives for pharmacologically refractory depression is an invasive direct electrical stimulation of relevant deep brain structures (20). Both unipolar and bipolar depression patients might benefit from deep brain stimulation (DBS) treatment (21), although an optimal approach, including selection of an optimal target structure, has yet to be established. To this end, the neuropathophysiology of depression needs to be better defined. Particularly, better understanding of connectivity properties of deep brain structures potentially implicated in DBS treatment could have an important value.

Neuroimaging techniques, such as fMRI and EEG analyses, let investigate the integration of functionally specialized brain regions in a network. Inferring the dynamical interactions among simultaneously recorded brain signals can reveal useful information in abnormal connectivity patterns due to pathologies and can help the clinical practice. The connectivity studies based on functional magnetic resonance imaging (fMRI) are most often based on correlation analyses without providing knowledge about the direction of the information flow between the examined regions. Directionality cannot be investigated using fMRI because of its poor temporal resolution (28). Understanding the directionality is, however, crucial when searching for suitable deep brain stimulation (DBS) targets for treating TRD. It was suggested that antidepressant effect of DBS treatment might be caused by changes in the activity of remote structures that receive inputs from the stimulated region. For instance, it has been hypothesized that DBS applied in the nucleus accumbens might influence the activity in the ventral (subgenual ACC, orbitofrontal and insular cortices) and dorsal (dorsal ACC, prefrontal and premotor cortices) subnetworks of the depression neurocircuitry (22). Another example of a particular role of the stimulated structure in the large-scale communication is the ACC, whose possible integrative role in cognitive processing (23) might explain the most recently reported high efficacy of DBS to subgenual ACC in treating depression (24).

The interest in studying the dynamical causal interactions that characterize rest- or task-related brain networks has led to a remarkable increase in the application of adaptive estimation algorithms. In particular, Granger causality based on adaptive filtering algorithms represents a suitable approach to study dynamical networks composed of highly non-stationary neural signals, e.g., EEG signals (25) (26). The adaptive filtering allows dealing with time-varying multivariate time-series and testing direct causal influences among brain regions. A signal x is said to Granger-cause another signal y if the history of x contains information that helps to predict y above and beyond the information contained in the history of y alone (27).

Aberrant functional EEG-based connectivity in depressive patients was reported in studies where network metrics were computed directly between sensor recordings (29)(30). Since each EEG channel is a linear mixture of concurrently active brain and non-brain electrical sources, whose activities are volume conducted to the scalp electrodes, the utility of such observations is limited (31). This EEG feature is particularly relevant in connectivity analyses which seek to detect the real

active interactions between brain regions. Connectivity analysis performed in the source space is able to partially overcome this issue (31). Indeed, Partial Directed Coherence estimators do not consider zero-lag interactions that describe the instantaneous propagation of activity, considering the zero-phase connectivity as noise added to lagged connectivity patterns of interest. For this reason, directed functional connectivity analysis based on electrical source imaging proved to be a promising tool to study the dynamics of spontaneous brain activity in healthy subjects and in various brain disorders (32) (33) (34). Despite this fact, the electromagnetic imaging has not been yet used in patients with depression to study the directed connectivity of resting-state networks.

In the current study, we explored the directed functional connectivity at rest in depression using high-density EEG. We computed the Partial Directed Coherence on the source EEG signals arising from the amygdala, anterior cingulate, putamen, pallidum, caudate, and thalamus, structures selected with respect to their potential implication in the DBS treating TRD. We hypothesized that the resting-state directed functional connectivity in these deep brain structures might be disrupted in patients with depression compared to healthy controls.

2 Methods

2.1 Subjects

Data was collected from 26 depressive patients and 25 healthy controls. The two groups were balanced in gender and there were no significant differences in age or education (see Table 1). On a subsample of this dataset we recently reported that the severity of depressive symptoms correlates with resting-state microstate dynamics (Damborská et al., under review). The patients were recruited by the Department of Psychiatry at the University Hospital Brno, Czech Republic, based on the clinical evaluation by two board-certified psychiatrists and according to the Diagnostic and Statistical Manual (DSM-V) criteria using the Mini International Neuropsychiatric interview (M.I.N.I.). All patients were examined during their first week of hospitalization. All patients met the criteria for at least a moderate degree of depression within the following affective disorders: bipolar affective disorder (F31), depressive episode (F32), and periodic depressive disorder (F33). Exclusion criteria for patients were any psychiatric or neurological comorbidity, IQ < 70, organic disorder with influence on the brain function, alcohol dependence or other substance dependence. All patients were in the on-medication state. Control subjects were recruited by general practitioners from their database of clients. Control subjects underwent the M.I.N.I. by board-certified psychiatrists, to ensure that they had no previous or current psychiatric disorder according to the DSM-V criteria. The scores on the Montgomery-Åsberg Depression Rating Scale (MADRS) (35) and the Clinical Global Impression (CGI) (36) tests were measured in patients to assess the severity of the depressive episode. The status of depression was further described with life time count of depressive episodes and illness duration. Medication in 24 hours preceding the EEG examination was also recorded (see Table 2). This study was carried out in accordance with the recommendations of Ethics Committee of University Hospital Brno with written informed consent from all subjects. All subjects gave written informed consent in accordance with the Declaration of Helsinki. The protocol was approved by the Ethics Committee of University Hospital Brno, Czech Republic.

2.2 EEG- data acquisition and pre-processing steps

Subjects were sitting in a comfortable upright position in an electrically shielded room with dimmed light. They were instructed to stay as calm as possible, to keep their eyes closed and to relax for 15 minutes. They were asked to stay awake. All participants were monitored by the cameras and in the event of signs of nodding off or EEG signs of drowsiness detected by visual inspection, the recording

was stopped. The EEG was recorded with a high density 128-channel system (EGI System 400; Electrical Geodesic Inc., OR, USA), f_s = 1kHz, and Cz as acquisition reference.

Five minutes of EEG data were selected and visually assessed. Noisy channels with abundant artifacts were identified. EEG signal was band-pass filtered between 1 and 40 Hz with a 2nd-order Butterworth filter avoiding phase-distortion. Subsequently, in order to remove physiological artifacts, e.g. ballistocardiogram and oculo-motor artifacts, infomax-based Independent Component Analysis (37) was applied on all but one or two noisy channels. Only components related to ballistocardiogram, saccadic eye movements, and eye blinking were removed based on the waveform, topography and time course of the component. Then, the cleaned EEG recording was down-sampled at f_s = 250 Hz and the previously identified noisy channels were interpolated using a three-dimensional spherical spline (38), and re-referenced to the average reference. For the following analyses, thirty 2-s EEG epochs free of artifacts were selected per subject. All the pre-processing steps were done using the freely available Cartool Software 3.70, programmed by Denis Brunet (39) and custom functions in MATLAB® R2018b.

2.3 EEG source estimation

We applied the LAURA algorithm implemented in Cartool (39) to compute the source reconstruction taking into account the patient's age to calibrate the skull conductivity (40)(41)(42). The method restricts the solution space to the gray matter of the brain. Then, the cortex was parcellated into the 90 Automated Anatomical Labeling brain regions (43). The dipoles in each region of interest (ROI) were represented with one unique time-series by a singular-value decomposition (44).

2.4 Time-variant multivariate autoregressive modeling

The cortical waveforms computed after applying the singular-value decomposition, were fitted against a time-variant (tv) multivariate (MV) autoregressive (AR) model to overcome the problem of non-stationarity of the EEG data. If the EEG data are available as several trials of the same length, the cortical waveforms computed from the EEG data generates a collection of realizations of a multivariate stochastic process which can be combined in a multivariate, multi-trial time series (44) (45) (46). The tv-MVAR matrices containing the model coefficients were computed in the framework of a MATLAB toolbox (code available upon reasonable request to the authors) that implements the adaptive Kalman filtering and information Partial Directed Coherence (iPDC) in the source space (46) (47) (48). By means of the model coefficients, we computed the parametric spectral power density and the iPDC absolute values for each subject. For each patient, we obtained a 4-dimensional matrix ([# ROIs x # ROIs x frequency x time]) that represented the directed information flow from one ROI to another for each frequency at each time sample. In this way we performed the analysis on the *single-subject* level.

Since the features in the power spectra were consistent among subjects in the same population (patients vs controls), we also performed the analysis on the *population* level. A *population subject* was built by estimating the tv-MVAR model, where each trial in input was a different subject. One power spectral density matrix and one connectivity matrix [ROIS x ROIs x frequency x time] were obtained for each group (controls and patients).

2.5 Network metrics

In order to study the peculiarities of the brain network in patients vs controls, the brain was represented as a digraph defined by a collection of nodes and directed links (directional edges). Nodes in the brain network represent brain regions, i.e., the 90 ROIs, while the directed links represent the values computed by iPDC. Thus, the weight of such link can vary in the interval [0-1]

and it represents the amount of mutual information flowing between ROIs. We defined twelve ROIs, including the bilateral amygdala, anterior cingulum, thalamus, putamen, caudate, and pallidum, to examine the directed functional connectivity between these seeds and the whole brain. Significant differences in power between patients and controls were observed in the *single-subject* level in alpha and theta frequency bands in all these six anatomical structures. Therefore, we restricted the network analysis to this [4-12] Hz frequency range. To evaluate how much the system is fault tolerant and how much the communication is efficient, the global efficiency for the whole brain and the local efficiency, clustering coefficient, strength and outflow for each of these twelve investigated ROIs were computed. To compute all the graph measures, the scripts and functions implemented on the freely available MATLAB toolbox (49) were customized.

2.5.1 Global efficiency

Global efficiency is defined as the average minimum path length between two nodes in the network. This measure is inversely related to topological distance between nodes and is typically interpreted as a measure of the capacity for parallel information transfer and integrated processing (50).

2.5.2 Local efficiency

Local efficiency is defined as the average efficiency of the local subgraphs (51), i.e. the global efficiency computed on the neighborhood of the node. It reflects the ability of a network to transmit information at the local level. This quantity plays a role similar to the clustering coefficient since it reveals how much the system is fault tolerant, i.e., it shows how efficient the communication is between the first neighbors of i when i is removed.

$$\overrightarrow{E_{loc}} = \frac{1}{2n}\sum_{i\in N}\frac{\sum_{j,h\in N, j\neq i}(a_{ij}+a_{ji})(a_{ih}+a_{hi})\left(\left[\overrightarrow{d_{jh}}(N_i)\right]^{-1}+\left[\overrightarrow{d_{hj}}(N_i)\right]^{-1}\right)}{\left(k_i^{out}+k_i^{in}\right)\left(k_i^{out}+k_i^{in}-1\right)-2\sum_{j\in N}a_{ij}a_{ji}} \quad (1)$$

where k_i^{out} is the out-degree of node i, k_i^{in} is the in-degree of node i, and a_{ij} is the connection status between node i and node j, i.e., $a_{ij} = 1$ if the link between i and j exists, $a_{ij} = 0$ otherwise. N is the set of nodes in the network. n is the number of nodes and $\overrightarrow{d_{jh}}(N_i)$ is the length of the shortest directed path between j (any node in the network) and h (any node that neighbors with i).

2.5.3 Clustering coefficient

Clustering coefficient reflects the prevalence of clustered connectivity around an individual brain region (52):

$$cc_i = \frac{2t_i}{k_i(k_i-1)} \quad (2)$$

where t_i are the number of triangles around the node i, and k_i is the degree of node i, i.e., the number of links connected to node i. In our case of a weighted directed network, a weighted directed version of clustering coefficient was used (53):

$$\overrightarrow{cc_i} = \frac{\overrightarrow{t_i}}{\left(k_i^{out}+k_i^{in}\right)\left(k_i^{out}+k_i^{in}-1\right)-2\sum_{j\in N}a_{ij}a_{ji}} \quad (3)$$

where $\overrightarrow{t_i}$ are the number of directed triangles around the node i, k_i^{out} is the out-degree of node i, k_i^{in} is the in-degree of node i, and a_{ij} is the connection status between the nodes i and j, i.e., $a_{ij} = 1$ if the link between i and j exists, $a_{ij} = 0$ otherwise. N is the set of nodes in the network.

2.5.4 Strength and outflow

Finally, the connectivity patterns between the different cortical regions were summarized by representing the strength that quantifies for each node the sum of weights of all links connected to the node and the total outflow from a region toward the others, generated by the sum of all the statistically significant links obtained by application of the iPDC. The greatest amount of information outflow depicts the ROI as one of the main sources (drivers) of functional connections to the other ROIs (54).

2.6 Laterality

For all the network metrics obtained in the previous paragraph, we also computed a laterality index, which is defined as $\frac{Left_{metric}-Right_{metric}}{Left_{metric}+Right_{metric}}$ to test if the measures significantly differentiate between the two hemispheres. Laterality index and all network metrics were calculated for both groups.

2.7 Statistical analysis

To assess whether or not the changes in the network metrics were statistically significant between patients and controls, paired Student's t-tests were computed under the hypothesis of normal distribution of samples (Lilliefors test), otherwise Wilcoxon rank-sign tests were considered. To test whether the age and education level predict the values of the spectral power distribution and the network metrics in patients, a multiple linear regression was performed. We also tested the influence of the clinical data on the connectivity results. A linear regression was performed exploiting correlation of the connectivity results with four variables describing the status of depression and two variables describing the medication status in terms of the intake of benzodiazepines (BZP), antidepressants, antipsychotics, and mood stabilizers (AD/AP/MS). These six clinical variables are provided for each patient in Table 2.

3 Results

3.1 Power spectra

We found an overall increase in power in theta and alpha frequency bands in patients compared to controls at both the *population* and *single-subject* levels. At the *population* level, significantly higher power ($p<0.05$) in patients was found in all investigated subcortical regions in both frequency bands (see Figure 1). At the *single-subject* level, a significantly higher power ($p<0.05$) in patients than in controls was observed in the [4-12] Hz frequency range bilaterally in the thalamus, pallidum, putamen, and caudate. Moreover, a significant left-lateralized power increase ($p<0.05$) in patients vs controls was observed in the anterior cingulate and amygdala in this frequency range (see Figure 2b). We found a significantly decreased power in delta and beta frequency bands in patients compared to controls in all investigated ROIs, when evaluating the results at the *population* level (Figure 1). At the *single-subject* level, delta power was significantly decreased in patients vs controls in the right caudate, putamen, and pallidum (Figure 2a). There was no significant difference in beta power between the two groups in any investigated ROI at the *single-subject* level (see Figure 2c).

3.2 Network metrics

The connectivity network measures that we performed in the [4-12] Hz frequency range, showed increased values in patients compared to controls at both levels. At the *population* level, the local efficiency measured in patients was higher than in controls in all examined subcortical ROIs (see

Figure 3). At the *single-subject* level, the global efficiency was significantly higher ($p<0.05$) in patients (mean $\pm$ standard deviation: 0.0129 ± 0.0021) than in controls (mean $\pm$ standard deviation: 0.0126 ± 0.0019). All the network measures computed on the twelve selected ROIs showed significantly higher values in patients than in controls in the right amygdala. The strength, local efficiency, and clustering coefficient of the right caudate were significantly higher in patients than controls, while there was no significant difference between the groups in the outflow from this ROI. There were no significant differences in any network metric in the anterior cingulate, thalamus, pallidum, or putamen (see Figure 4).
There were no statistical differences in the network metrics estimated between the left and right hemisphere in each subject. The laterality indices showed that neither controls, nor patients had a lateralization in connectivity results of the six investigated deep brain structures. No significant differences in the laterality indices were observed comparing controls and patients.

3.3 Effect of medication on network impairments

We found no correlation of the connectivity results with the intake of benzodiazepines, while there was a significant relationship between the global efficiency and the intake of AD/AP/MS medication ($R^2 = 0.59$ and $p_{value} = 1.52\text{e} - 05$). The global efficiency decreased with increasing medication score (see Figure 5). We observed no significant correlation ($R^2 < 0.05$ and $p_{value} > 0.8$) between the connectivity results and any of the parameters that describe the status of depression (MADRS score, CGI score, illness duration, and the number of episodes) or the demographic profile (age and education level).

Figure 1

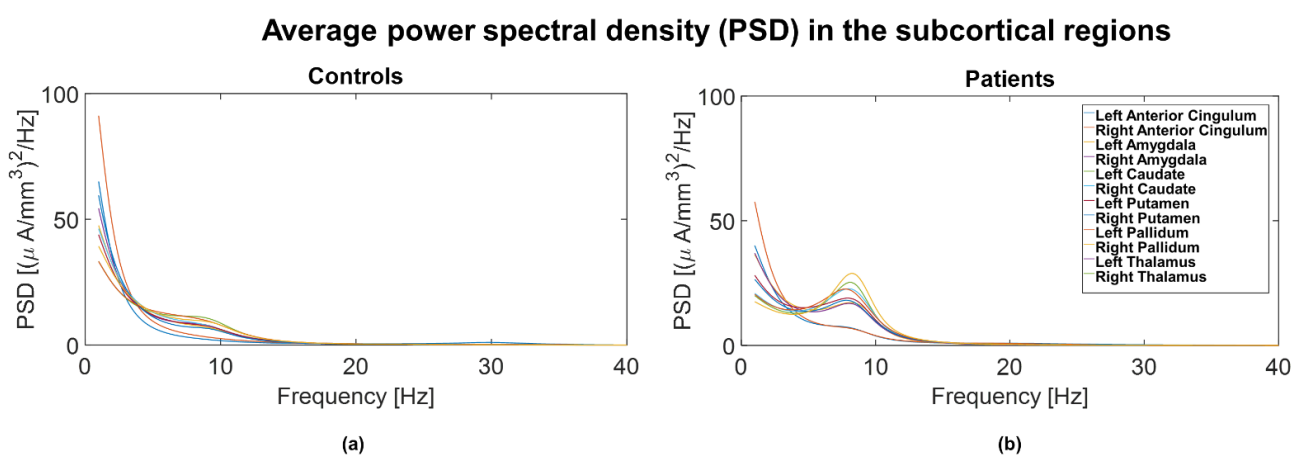

Figure 2

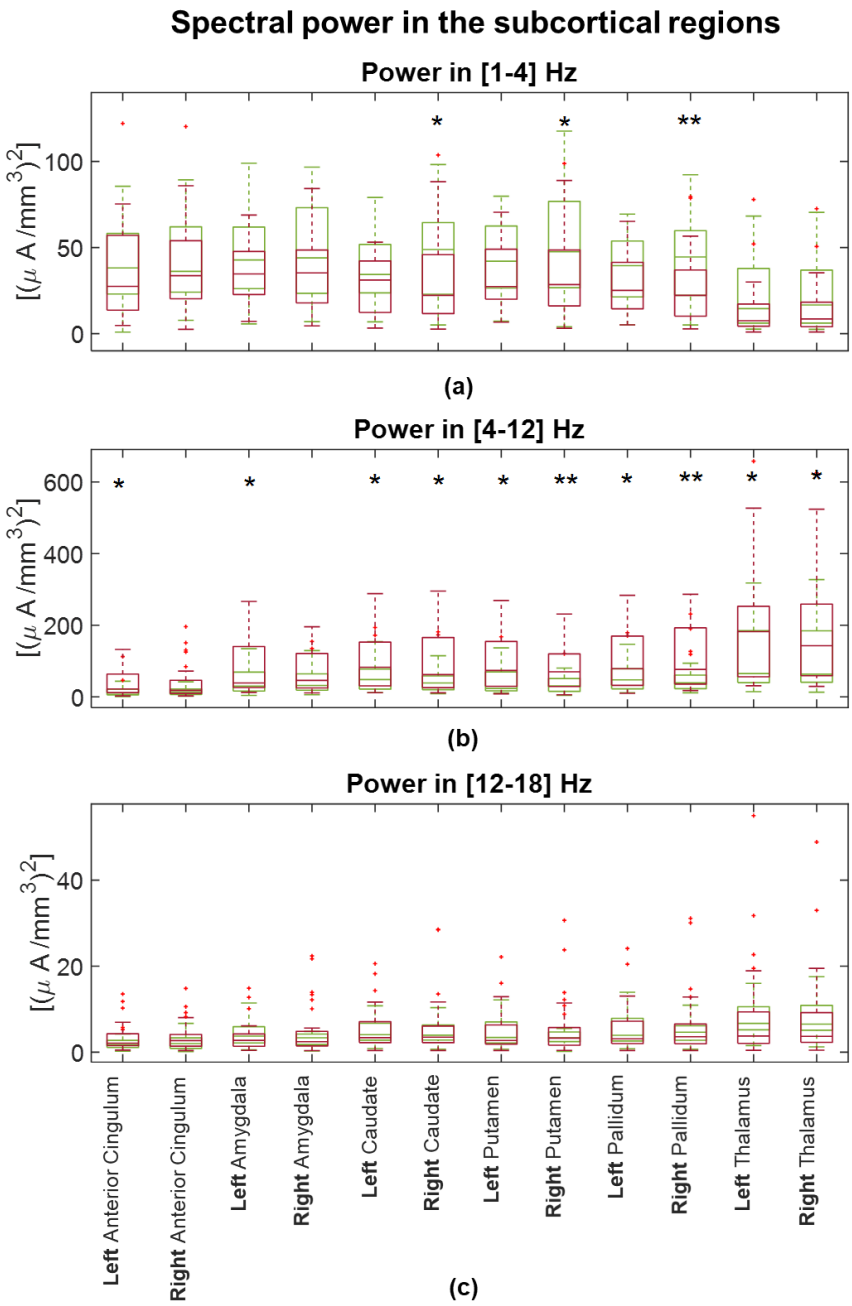
Spectral power in the subcortical regions
Power in [1-4] Hz
[(μ A /mm3)2]
(a)
Power in [4-12] Hz
[(μ A /mm3)2]
(b)
Power in [12-18] Hz
[(μ A /mm3)2]
Left Anterior Cingulum
Right Anterior Cingulum
Left Amygdala
Right Amygdala
Left Caudate
Right Caudate
Left Putamen
Right Putamen
Left Pallidum
Right Pallidum
Left Thalamus
Right Thalamus
(c)

Figure 3

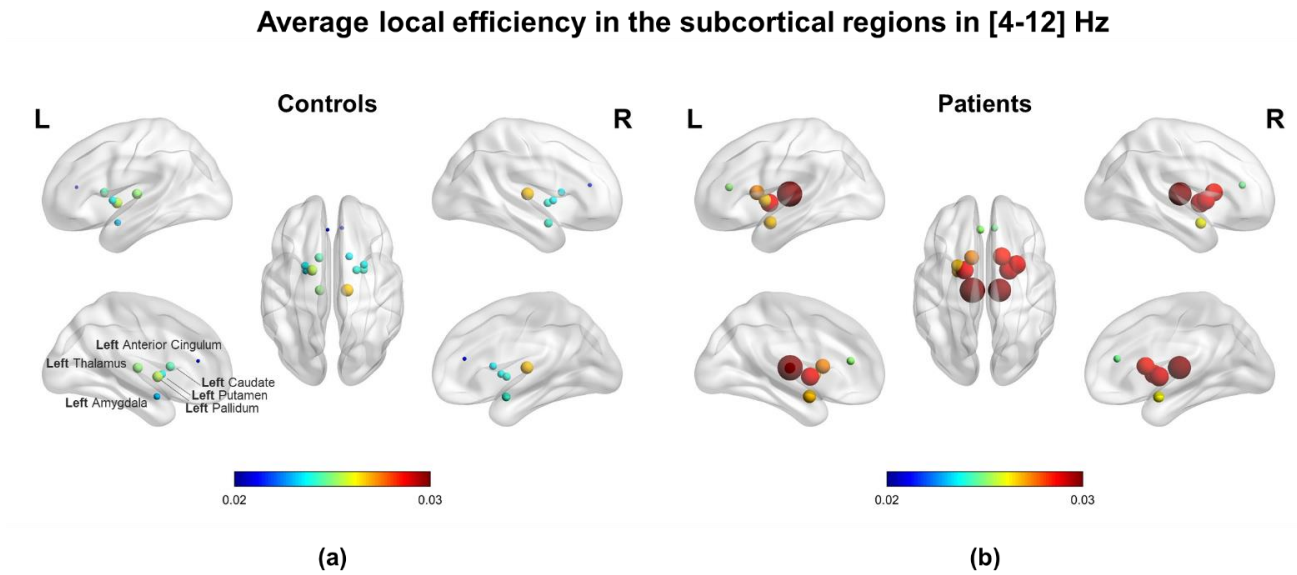

Figure 4

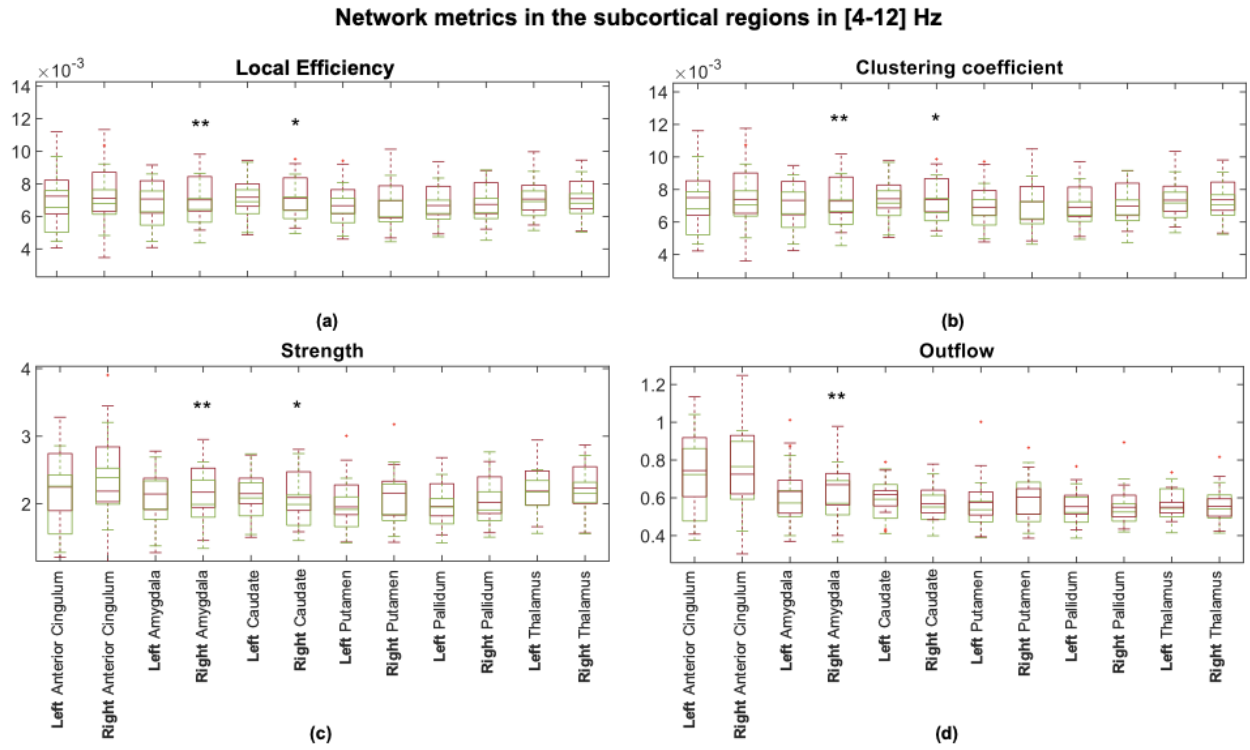

Figure 5

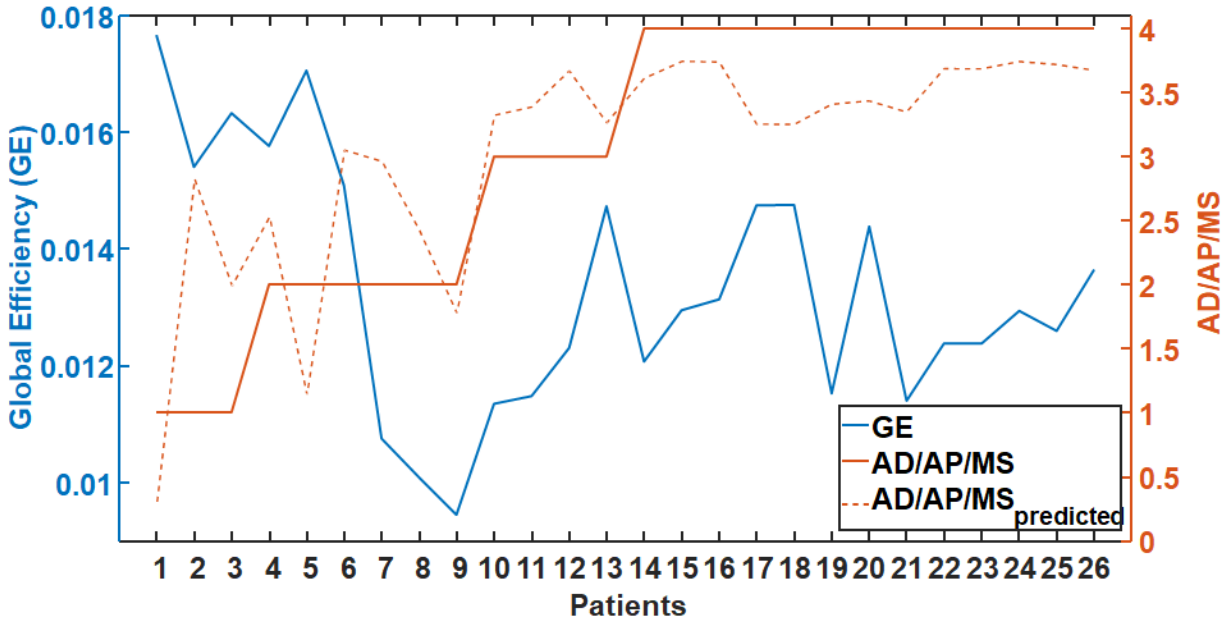

4 Discussion

In this study, we investigated resting-state network alterations using iPDC on source signals of high-density EEG in patients with depression compared to healthy controls. We explored the directed functional connectivity of the amygdala, anterior cingulate, putamen, pallidum, caudate, and thalamus, among them and with all the other brain regions. We demonstrated that in patients with moderate to severe depression: (1) the directed functional connectivity was significantly increased compared to controls in the right amygdala and the right caudate; (2) the power in theta and alpha frequency bands was significantly increased compared to controls in all investigated brain anatomical structures; (3) higher medication intake was associated with lower overall driving from the investigated regions.

4.1 Increased right amygdala directed functional connectivity in depression

The most robust finding in our study was an abnormally increased directed functional connectivity in the right amygdala during resting-state in depressive patients. Even though the left-right asymmetry was not demonstrated by the LI, a right-lateralized hyper-connectivity, as revealed with all the computed network metrics, was observed in the amygdala. We observed an increase in outgoing connections from the right amygdala as reflected with significantly higher outflow and strength in patients compared to controls. Moreover, we found a hyper-connectivity in the local networks of the right amygdala as reflected with significantly higher local efficiency and clustering coefficient in patients compared to controls.

We also found a significantly higher global efficiency in patients compared to healthy controls. This network feature had the same trend at the *population* level. Namely, we observed abnormally increased local efficiency of all examined deep brain structures in depressive patients. The efficiency measures the ability of a neural network to integrate and combine information. The deeper regions

have a key role as hubs of the large-scale brain networks, so changes in their local connectivity properties might have also led to connectivity changes in the whole brain.

The amygdala is involved in processing salient stimuli (55)(56) and has been implicated as one of the central hubs within the affective salience network (57)(58)(59). There is converging evidence from the neuroimaging studies that points to an abnormally increased connectivity and heightened activation of the amygdala in major depressive disorder (MDD) patients (60)(61), although reduced connectivity was also reported (62)(17)(63). Distinct network dysfunctions in MDD were suggested to underlie adult-specific amygdala resting-state fMRI connectivity impairment within the affective network, presumably reflecting an emotional dysregulation in MDD (64). Unfortunately, the directionality of connections, which might be of interest when considering a structure as a potential DBS-target for treatment of TRD, cannot be inferred from these functional studies. Here, we demonstrated in depressive patients an abnormal increase in directed functional connectivity arising from the right amygdala. This higher connectivity could reflect abnormal functioning of the right amygdala in terms of the hyper-activation. Such dysfunction might represent an impaired bottom-up signaling for top-down cortical modulation of limbic regions, leading to an abnormal affect regulation in these patients.

The increased functional connectivity in amygdala is likely related to structural changes observed in depression. Enlarged amygdala volume was found in first-episode depressive patients that positively correlated with severity of depression (65). Higher grey matter volume was detected in bilateral amygdala of TRD patients compared to non-TRD patients, irrespective whether the patients presented bipolar or unipolar features (66). Decreased amygdala volumes have also been reported in first-episode depressive patients (2). Larger amygdala volumes were suggested to reflect vulnerability to chronicity, revealed by medication resistance (66) or a consequence of progression of the disorder (2). On the other hand, larger right amygdala volume was suggested to be associated with greater chances of remission in BD (67).

In our study we aimed to investigate the directed functional connectivity in amygdala to provide knowledge on neurobiology of depression that is needed for evaluation this structure as a possible candidate for DBS treatment in depression. Despite myriad of DBS targets for treating depression tested in humans (20), the amygdala is not among them. The possible safety and utility of DBS in the amygdala could only be inferred from studies, in which the amygdala-DBS was performed for other neuropsychiatric diagnoses, such as epilepsy (68)(69)(70)(71), post-traumatic stress disorder (72)(73), and autism (74). In one of these studies transient stimulation-related positive shift in mood was observed (69). Particularly, the stimulation of the right amygdala induced a transient decrease in the negative affective bias, i.e. the tendency to interpret ambiguous or positive events as relatively negative. In this case study, an epileptic patient with MDD rated the emotional facial expressions as more positive with stimulation than without. The stimulation effect might have been associated with a transient normalization of likely impaired function of the right amygdala in that patient. We can only speculate, whether this dysfunction was in terms of hyper-connectivity similar to that observed in our study and whether it was temporally decreased by inhibitory effect of the stimulation. Nevertheless, if this was the case, results of that case study together with the here reported right-lateralized hyper-connectivity in depressive patients would support the right amygdala as a candidate future DBS target for treating TRD.

4.2 Increased right caudate directed functional connectivity in depression

We demonstrated that during resting state, patients had significantly higher right caudate directed functional connectivity than healthy controls. Despite no significant difference between groups in

the caudate outflow, we observed an abnormally increased strength of outgoing connections from the right caudate in patients. Moreover, we found a hyper-connectivity in the local networks of the right caudate as reflected with significantly higher local efficiency and clustering coefficient in patients compared to controls. These findings might be consistent with evidence directly associating cortico-basal ganglia pathology with primary bipolar and unipolar spectrum disorders (75). Deficits in resting-state default-mode network connectivity with the bilateral caudate were suggested to be an early manifestation of MDD (76). Reduced grey matter volume in the bilateral caudate (77)(78)(79)(12) and altered functional connectivity of the right caudate with the frontal regions was observed in MDD patients (78). In a post-mortem morphometric study in late-life depressive subjects, reduction in neuronal density was found in both the dorsolateral and ventromedial areas of the caudate nucleus (80). Negative association between increased white matter lesion volumes and decreased right caudate volume in late-life depression was reported (81). In mild to moderately depressed patients no change in caudate gray matter volumes were found (82) suggesting inverse correlation between the caudate volume and severity of depression.

No significant differences in any network metric were found in the putamen, pallidum, thalamus, and anterior cingulate. It is possible, however, that examining these structures as a whole might be insensitive to different changes in their relevant subregions. Only medial part of thalamus is expected to play a role in the experience of affect (60)(83). Reduced activity in the dorsal ACC but increased activity in the subgenual ACC have been found in acute depression in functional imaging studies (84)(85). Moreover, we must take into account the limitations of our methodological approach, i.e. the source localization of the EEG activity in the subcortical regions. Despite, it was recently proved that subcortical activity is detectable with high density EEG (86), we have to keep in mind that the spatial resolution in detecting and distinguishing neighboring brain regions is about 24 mm. Therefore, our results divided into caudate, putamen and pallidum are probably overlapping. Keeping in mind these limitations and with respect to the lower robustness of our findings in the caudate, we can just encourage researchers to further investigate the dysfunction of the caudate nucleus in depression so that any conclusions about its suitability as a DBS target for treating depression can be made. In an early case study, stimulation of the ventral caudate nucleus markedly improved symptoms of depression in a patient with MDD and comorbid obsessive-compulsive disorder (87). No change in depressive symptoms, however, was recently observed during the stimulation of the caudate in a study of three TRD patients (88) and authors concluded the caudate to be less promising target than the nucleus accumbens. More evidence from neuroimaging studies is needed to provide arguments for the next caudate-DBS tests in treating TRD.

4.3 Increased theta and alpha powers in depression

We found a significantly higher power in the theta and alpha frequency bands in the depressed compared to healthy control group in all the investigated subcortical structures consistently at both the *population* and *single-subject* levels. The power decrease in the beta and delta frequency bands was observed only in the right striatum at both levels.

Our findings might be in line with previous observations in the sensor space of the scalp EEG. Abnormally high power in alpha (89)(90)(91) and theta (89)(92)(91) frequency bands in parietal and occipital regions were found in depressed patients, lower than normal beta and delta power were also reported (91). The recent evidence points, however, to opposite power changes showing that theta and alpha power might decrease, while beta power increase in depression (93). Moreover, the same study reported negative association of the posterior alpha power with the depression severity. While changes in cortical theta and alpha activity were suggested to be inversely related to the level of

cortical activation, enhancement of the cortical beta power was suggested to reflect higher level of anxiety symptoms in depressed patients (89). To the best of our knowledge there is only one study that directly recorded electrophysiological activity in subcortical structures in depressive patients. In this study, a larger alpha activity in MDD patients compared with obsessive compulsive disorder was found in the limbic DBS targets (the anterior cingulate and the bed nucleus of the stria terminalis) (94). Moreover, in the same study, the increased alpha power correlated with severity of depressive symptoms. Nevertheless, in spite of parallels with prior reports, the current link between the power changes in subcortical structures and depression awaits replication.

4.4 Lower network impairments with more medication

We found an inverse relationship between the intake of medication and the impairment of the investigated networks. Particularly, increased intake of antidepressants, antipsychotics, and mood stabilizers was associated with reduction of the global efficiency. This finding might be related to the pharmacological effect on the brain activity, i.e. a change towards the normalization of the hyper-connectivity in the cortico-striatal-pallidal-thalamic and limbic networks. Although, only doses of medication actually taken at the time of experiment were considered, the accumulated drug effect on connectivity results might be also expected. The low sample size and great variability in medication made it, however, impossible to examine any potential influence of medication on the network impairments by comparing patients receiving a specific drug with those not receiving it. To summarize the various medications, an ordinal variable was used that is only a rough measurement of medication usage. Therefore, the observed relationship between the global efficiency and medication should be viewed with caution. Interestingly, we have not found significant correlation between the global efficiency and intake of benzodiazepines. This negative finding suggests that even though benzodiazepines are known to have an effect on electrophysiological correlates of brain functions, the network properties might not be influenced. There were no significant correlations between the connectivity results and symptom severity or other parameters describing the status of depression within the patient group. We suppose that heterogeneity of our dataset, in which patients with different disorders were included, might underlie this observation.

5 Conclusions

We found an overall increase in power in theta and alpha frequency bands in depressive patients compared to healthy controls in the subcortical regions constituting the cortico-striatal-pallidal-thalamic and limbic circuits. The network measures showed a higher than normal functional connectivity arising from the right amygdala in depressive patients. The amygdala seems to play an important role in neurobiology of depression and as such could be considered as a potential future target for DBS in treating TRD. The observed right-lateralized alterations in the brain connectivity support the unilateral approach in neurostimulation treatment of depression. Resting-state EEG directed functional connectivity is a useful tool for studying abnormal brain activity in depression.

6 Table legends

Table 1. [a]Education was classified into three levels: 1 = no high school, 2 = high school, 3 = university studies

Table 2. F31: bipolar affective disorder; F32: depressive episode, F33: periodic depressive disorder; BZD: benzodiazepine equivalent dose(95); AD/AP/MS (antidepressants/antipsychotics/mood stabilizers): 1 – one medication in sub-therapeutic doses, 2 – one medication in therapeutic doses, 3 – combination of medications with one in therapeutic doses, 4 – combination of medications with more

than one in therapeutic doses; MADRS: Montgomery–Åsberg Depression Rating Scale; CGI (Clinical Global Impression scale): healthy (1) – most extremely ill (7). Patients 3, 4, and 9 received electroconvulsive therapy; patient 5 received transcranial magnetic stimulation.

7 Tables

Table 1. Demographic data

Characteristic	Patients (n = 26)	Controls (n = 25)	*t*-value	df	p-value
Age: mean ± SD	51.9 ± 9.1	49.5 ± 8.7	0.97	49	0.34
Gender: female, *n*	11	10			
Education[a]: mean ± SD	1.9 ± 0.9	2.3 ± 0.7	-1.70	49	0.10

Table 2. Patient characteristics

Patient	Diagnose	Number of episodes	Illness duration (years)	MADRS score	CGI score	BZD	AD/AP/MS
1	F31	3	2	27	4	2	3
2	F32	1	0.5	24	5	0	2
3	F32	1	1	15	4	2	2
4	F31	5	20	39	6	0	2
5	F33	3	7	18	4	0	1
6	F33	2	8	9	3	1.33	1
7	F32	1	1	24	4	1.33	3
8	F31	4	27	29	5	2	2
9	F33	2	5	36	6	1	4
10	F33	3	19	21	4	1	1
11	F33	2	2	38	5	6	4
12	F33	2	1	39	5	3	4
13	F32	1	0.08	21	5	2	4
14	F33	5	21	32	5	0	3
15	F33	2	2	38	6	3	4
16	F32	1	0.08	37	6	2	4
17	F33	3	4	18	4	0	4
18	F31	2	16	28	4	0	4

19	F31	11	24	23	4	1	4
20	F32	0	0,17	23	4	1	4
21	F33	1	9	34	5	2	2
22	F32	0	0,04	37	6	1	4
23	F33	1	11	49	6	3	4
24	F33	3	20	23	4	0	2
25	F33	5	24	26	4	2	4
26	F32	0	0,17	23	4	3	3

8 Figure legends

Figure 1 Parametric power spectral density (PSD) of the *population subjects* representing controls (a) vs patients (b) in the subcortical regions of interest. Power significantly increases in theta ([4-8] Hz) and alpha ([8-12] Hz) band and decreases in delta ([1-4] Hz) and beta ([12-18] Hz) bands in patients compared to controls ($p<0.05$) in the subcortical regions of interest.

Figure 2 Boxplots to graphical illustrate the distribution of power of controls (green boxes) and patients (red boxes) in (a) [1-4] Hz, (b) [4-12] Hz and (c) [12-18] Hz. One star (*) stands for significant statistical difference with $p<0.05$ and two stars (**) for $p<0.001$. Power in [4-12] Hz significantly increases in patients compared to controls in all examined anatomical brain structures.

Figure 3 Local efficiency computed in the two *population subjects* representing (a) controls and (b) patients. The efficiency for each ROI is represented by a sphere centered on the cortical region, whose radius is linearly related to the magnitude. Such information is also coded through a color scale. The local efficiency, i.e., the ability of a network to transmit information at the local level, measured in patients is higher than in controls in all the subcortical regions of interest.

Figure 4 Boxplots to graphically illustrate the distribution of (a) local efficiency, (b) clustering coefficient, (c) strength, and (c) outflow in controls (green boxes) and patients (red boxes). One star (*) stands for significant statistical difference with $p<0.05$ and two stars (**) for $p<0.001$. All network metrics that refer to the right amygdala significantly differ between controls and patients ($p<0.001$).

Figure 5 Relationship between the intake of antidepressants/antipsychotics/mood stabilizers (AD/AP/MS) and the global efficiency (GE). Note that higher medication intake is associated with lower GE. The orange dotted line stands for the predicted value of AD/AP/MS for each patient using GE as predictor.

9 Conflict of Interest

The authors declare that the research was conducted in the absence of any commercial or financial relationships that could be construed as a potential conflict of interest.

10 Author Contributions

AD – designed the study, performed the preprocessing, and wrote the initial draft; MR – performed the analysis and wrote the initial draft; RB and JH – were responsible for patient recruitment and clinical assessment; EH – collected the EEG data; SF and ŠO – were involved in the clinical assessment; CM – served as an advisor and was responsible for the overall oversight of the study. All authors revised the manuscript.

11 Funding

This project received funding from the European Union Horizon 2020 research and innovation program under the Marie Skłodowska-Curie grant agreement No. 739939. The study was also supported by Ministry of Health, Czech Republic - conceptual development of research organization (University Hospital Brno - FNBr, 65269705). These funding sources had no role in the design, collection, analysis, or interpretation of the study.

12 Acknowledgments

The authors wish to thank Anne Meredith Johnson for providing language help.

13 References

1. Andrade L, Caraveo-anduaga JJ, Berglund P, Bijl R V., Graaf R De, Vollebergh W, et al. The epidemiology of major depressive episodes: results from the International Consortium of Psychiatric Epidemiology (ICPE) surveys. Int J Methods Psychiatr Res [Internet]. 2003 Feb [cited 2019 Apr 11];12(1):3–21. Available from: http://doi.wiley.com/10.1002/mpr.138

2. Bora E, Harrison BJ, Davey CG, Yü Cel M, Pantelis C. Meta-analysis of volumetric abnormalities in cortico-striatal-pallidal-thalamic circuits in major depressive disorder. [cited 2019 Apr 2]; Available from: https://search-proquest-com.ezproxy.muni.cz/docview/1266777617/fulltextPDF/B83579CA61C445F7PQ/1?accountid=16531

3. Yang J, Yin Y, Svob C, Long J, He X, Zhang Y, et al. Amygdala Atrophy and Its Functional Disconnection with the Cortico-Striatal-Pallidal-Thalamic Circuit in Major Depressive Disorder in Females. Hayasaka S, editor. PLoS One [Internet]. 2017 Jan 20 [cited 2019 Apr 9];12(1):e0168239. Available from: http://dx.plos.org/10.1371/journal.pone.0168239

4. Zhang B, Lin P, Shi H, Öngür D, Auerbach RP, Wang X, et al. Mapping anhedonia-specific dysfunction in a transdiagnostic approach: an ALE meta-analysis. Brain Imaging Behav [Internet]. 2016 Sep 20 [cited 2019 Apr 10];10(3):920–39. Available from: http://link.springer.com/10.1007/s11682-015-9457-6

5. Disner SG, Beevers CG, Haigh EAP, Beck AT. Neural mechanisms of the cognitive model of depression. Nat Rev Neurosci [Internet]. 2011 Jul 6 [cited 2019 Apr 11];12(8):467–77. Available from: http://www.nature.com/doifinder/10.1038/nrn3027

6. Surguladze S, Brammer MJ, Keedwell P, Giampietro V, Young AW, Travis MJ, et al. A differential pattern of neural response toward sad versus happy facial expressions in major depressive disorder. Biol Psychiatry [Internet]. 2005 Feb [cited 2019 Apr 10];57(3):201–9. Available from: https://linkinghub.elsevier.com/retrieve/pii/S0006322304011084

7. Sheline YI, Barch DM, Donnelly JM, Ollinger JM, Snyder AZ, Mintun MA. Increased amygdala response to masked emotional faces in depressed subjects resolves with antidepressant treatment: an fMRI study. Biol Psychiatry [Internet]. 2001 Nov [cited 2019 Apr 10];50(9):651–8. Available from: http://linkinghub.elsevier.com/retrieve/pii/S000632230101263X

8. Siegle GJ, Thompson W, Carter CS, Steinhauer SR, Thase ME. Increased Amygdala and Decreased Dorsolateral Prefrontal BOLD Responses in Unipolar Depression: Related and Independent Features. Biol Psychiatry [Internet]. 2007 Jan [cited 2019 Apr 11];61(2):198–209. Available from: https://linkinghub.elsevier.com/retrieve/pii/S0006322306007931

9. Nugent AC, Robinson SE, Coppola R, Furey ML, Zarate CA. Group differences in MEG-ICA derived resting state networks: Application to major depressive disorder. Neuroimage [Internet]. 2015 Sep [cited 2019 Apr 11];118:1–12. Available from: https://linkinghub.elsevier.com/retrieve/pii/S1053811915004334

10. Knyazev GG, Savostyanov AN, Bocharov A V., Brak I V., Osipov EA, Filimonova EA, et al. Task-positive and task-negative networks in major depressive disorder: A combined fMRI and EEG study. J Affect Disord [Internet]. 2018 Aug [cited 2019 Apr 11];235:211–9. Available from: https://linkinghub.elsevier.com/retrieve/pii/S0165032717321341

11. Lu Y, Liang H, Han D, Mo Y, Li Z, Cheng Y, et al. The volumetric and shape changes of the putamen and thalamus in first episode, untreated major depressive disorder. NeuroImage Clin [Internet]. 2016 [cited 2019 Apr 11];11:658–66. Available from: http://www.ncbi.nlm.nih.gov/pubmed/27222797

12. Kim MJ, Hamilton JP, Gotlib IH. Reduced caudate gray matter volume in women with major depressive disorder. Psychiatry Res Neuroimaging [Internet]. 2008 Nov [cited 2019 Apr 10];164(2):114–22. Available from: https://linkinghub.elsevier.com/retrieve/pii/S0925492707002661

13. Sheline YI, Price JL, Yan Z, Mintun MA. Resting-state functional MRI in depression unmasks increased connectivity between networks via the dorsal nexus. Proc Natl Acad Sci [Internet]. 2010 Jun 15 [cited 2019 Apr 11];107(24):11020–5. Available from: http://www.pnas.org/cgi/doi/10.1073/pnas.1000446107

14. Kuhn S, Gallinat J. Resting-State Brain Activity in Schizophrenia and Major Depression: A Quantitative Meta-Analysis. Schizophr Bull [Internet]. 2013 Mar 1 [cited 2019 Apr 11];39(2):358–65. Available from: https://academic.oup.com/schizophreniabulletin/article-lookup/doi/10.1093/schbul/sbr151

15. Lorenzetti V, Allen NB, Fornito A, Yücel M. Structural brain abnormalities in major depressive disorder: A selective review of recent MRI studies. J Affect Disord [Internet]. 2009 Sep [cited 2019 Apr 11];117(1–2):1–17. Available from: https://linkinghub.elsevier.com/retrieve/pii/S016503270800476X

16. Veer IM. Whole brain resting-state analysis reveals decreased functional connectivity in major depression. Front Syst Neurosci [Internet]. 2010 [cited 2019 Apr 11];4. Available from: http://journal.frontiersin.org/article/10.3389/fnsys.2010.00041/abstract

17. Hamilton JP, Etkin A, Furman DJ, Lemus MG, Johnson RF, Gotlib IH. Functional Neuroimaging of Major Depressive Disorder: A Meta-Analysis and New Integration of Baseline Activation and Neural Response Data. Am J Psychiatry [Internet]. 2012 Jul [cited 2019 Apr 2];169(7):693–703. Available from: http://psychiatryonline.org/doi/abs/10.1176/appi.ajp.2012.11071105

18. Bielau H, Trübner K, Krell D, Agelink MW, Bernstein H –G., Stauch R, et al. Volume deficits of subcortical nuclei in mood disorders. Eur Arch Psychiatry Clin Neurosci [Internet]. 2005 Dec 17 [cited 2019 Apr 11];255(6):401–12. Available from: http://link.springer.com/10.1007/s00406-005-0581-y

19. Holtzheimer PE, Mayberg HS. Stuck in a rut: rethinking depression and its treatment. Trends Neurosci [Internet]. 2011 Jan [cited 2019 Apr 11];34(1):1–9. Available from: https://linkinghub.elsevier.com/retrieve/pii/S0166223610001530

20. Drobisz D, Damborská A. Deep brain stimulation targets for treating depression. Behav Brain Res [Internet]. 2019 Feb;359:266–73. Available from: https://linkinghub.elsevier.com/retrieve/pii/S0166432818307344

21. Holtzheimer PE, Kelley ME, Gross RE, Filkowski MM, Garlow SJ, Barrocas A, et al. Subcallosal Cingulate Deep Brain Stimulation for Treatment-Resistant Unipolar and Bipolar Depression. Arch Gen Psychiatry [Internet]. 2012 Feb 1 [cited 2019 Apr 3];69(2):150. Available from: http://archpsyc.jamanetwork.com/article.aspx?doi=10.1001/archgenpsychiatry.2011.1456

22. Kopell BH, Greenberg B, Rezai AR. Deep Brain Stimulation for Psychiatric Disorders. J Clin Neurophysiol [Internet]. 2004 Jan [cited 2019 Apr 11];21(1):51–67. Available from: http://content.wkhealth.com/linkback/openurl?sid=WKPTLP:landingpage&an=00004691-200401000-00007

23. Kukleta M, Bob P, Brázdil M, Roman R, Rektor I. The level of frontal-temporal beta-2 band EEG synchronization distinguishes anterior cingulate cortex from other frontal regions. Conscious Cogn [Internet]. 2010 Dec [cited 2019 Apr 11];19(4):879–86. Available from: https://linkinghub.elsevier.com/retrieve/pii/S1053810010000796

24. Kibleur A, Polosan M, Favre P, Rudrauf D, Bougerol T, Chabardès S, et al. Stimulation of subgenual cingulate area decreases limbic top-down effect on ventral visual stream: A DBS-EEG pilot study. Neuroimage [Internet]. 2017 Feb [cited 2019 Apr 11];146:544–53. Available from: https://linkinghub.elsevier.com/retrieve/pii/S1053811916305729

25. Pereda E, Quiroga RQ, Bhattacharya J. Nonlinear multivariate analysis of neurophysiological signals. Prog Neurobiol [Internet]. 2005 Sep [cited 2019 Apr 16];77(1–2):1–37. Available from: https://linkinghub.elsevier.com/retrieve/pii/S030100820500119X

26. Seth AK, Barrett AB, Barnett L. Granger Causality Analysis in Neuroscience and Neuroimaging. J Neurosci [Internet]. 2015 Feb 25 [cited 2019 Apr 16];35(8):3293–7. Available from: http://www.jneurosci.org/cgi/doi/10.1523/JNEUROSCI.4399-14.2015

27. Granger CWJ. Investigating Causal Relations by Econometric Models and Cross-spectral Methods. Econometrica. 1969;37(3):424–38.

28. Smith SM, Miller KL, Salimi-Khorshidi G, Webster M, Beckmann CF, Nichols TE, et al. Network modelling methods for FMRI. Neuroimage [Internet]. 2011 Jan [cited 2019 Apr 9];54(2):875–91. Available from: https://linkinghub.elsevier.com/retrieve/pii/S1053811910011602

29. Leistritz L, Weiss T, Ionov J, Bär K-J, Miltner WHR, Witte H. Connectivity Analysis of Somatosensory Evoked Potentials in Patients with Major Depression. Methods Inf Med [Internet]. 2010 Jan 17 [cited 2019 Apr 9];49(05):484–91. Available from: http://www.thieme-connect.de/DOI/DOI?10.3414/ME09-02-0038

30. Yu Sun, Sijung Hu, Chambers J, Yisheng Zhu, Shanbao Tong. Graphic patterns of cortical functional connectivity of depressed patients on the basis of EEG measurements. In: 2011 Annual International Conference of the IEEE Engineering in Medicine and Biology Society [Internet]. IEEE; 2011 [cited 2019 Apr 9]. p. 1419–22. Available from: http://ieeexplore.ieee.org/document/6090334/

31. Schoffelen J-M, Gross J. Source connectivity analysis with MEG and EEG. Hum Brain Mapp [Internet]. 2009 Jun [cited 2019 Apr 9];30(6):1857–65. Available from: http://doi.wiley.com/10.1002/hbm.20745

32. Coito A, Michel CM, van Mierlo P, Vulliemoz S, Plomp G. Directed Functional Brain Connectivity Based on EEG Source Imaging: Methodology and Application to Temporal Lobe Epilepsy. IEEE Trans Biomed Eng [Internet]. 2016 Dec [cited 2019 Apr 9];63(12):2619–28. Available from: http://ieeexplore.ieee.org/document/7604056/

33. Sperdin HF, Coito A, Kojovic N, Rihs TA, Jan RK, Franchini M, et al. Early alterations of social brain networks in young children with autism. Elife [Internet]. 2018 Feb 27 [cited 2019 Apr 9];7. Available from: https://elifesciences.org/articles/31670

34. Coito A, Michel CM, Vulliemoz S, Plomp G. Directed functional connections underlying spontaneous brain activity. Hum Brain Mapp [Internet]. 2019 Feb 15 [cited 2019 Apr 9];40(3):879–88. Available from: http://doi.wiley.com/10.1002/hbm.24418

35. Williams JBW, Kobak KA. Development and reliability of a structured interview guide for the Montgomery-Åsberg Depression Rating Scale (SIGMA). Br J Psychiatry [Internet]. 2008 Jan 2 [cited 2019 Mar 29];192(01):52–8. Available from: https://www.cambridge.org/core/product/identifier/S0007125000248447/type/journal_article

36. Guy W. ECDEU assessment manual for psychopharmacology [Internet]. Rev. Rockville Md.: U.S. Dept. of Health Education and Welfare Public Health Service Alcohol Drug Abuse and Mental Health Administration National Institute of Mental Health Psychopharmacology Research Branch; 1976 [cited 2019 Mar 29]. Available from: https://www.worldcat.org/title/ecdeu-assessment-manual-for-psychopharmacology/oclc/2344751

37. Jung T-P, Makeig S, Westerfield M, Townsend J, Courchesne E, Sejnowski TJ. Removal of eye activity artifacts from visual event-related potentials in normal and clinical subjects. Clin Neurophysiol [Internet]. 2000 Oct [cited 2019 Mar 29];111(10):1745–58. Available from: http://linkinghub.elsevier.com/retrieve/pii/S1388245700003862

38. Perrin F, Pernier J, Bertrand O, Echallier JF. Spherical splines for scalp potential and current density mapping. Electroencephalogr Clin Neurophysiol [Internet]. 1989 Feb [cited 2019 Mar 29];72(2):184–7. Available from: https://linkinghub.elsevier.com/retrieve/pii/0013469489901806

39. "the Cartool Community group," [Online]. Available: cartoolcommunity.unige.ch.

40. Grave de Peralta Menendez R, Murray MM, Michel CM, Martuzzi R, Gonzalez Andino SL. Electrical neuroimaging based on biophysical constraints. Neuroimage [Internet]. 2004 Feb 1 [cited 2019 Mar 13];21(2):527–39. Available from: https://www.sciencedirect.com/science/article/pii/S1053811903006013

41. Brunet D, Murray MM, Michel CM. Spatiotemporal Analysis of Multichannel EEG: CARTOOL. Comput Intell Neurosci [Internet]. 2011 [cited 2019 Mar 13];2011:1–15. Available from: http://www.hindawi.com/journals/cin/2011/813870/

42. Spinelli L, Andino SG, Lantz G, Seeck M, Michel CM. Electromagnetic Inverse Solutions in Anatomically Constrained Spherical Head Models. Brain Topogr [Internet]. 2000 [cited 2019 Mar 13];13(2):115–25. Available from: http://link.springer.com/10.1023/A:1026607118642

43. Tzourio-Mazoyer N, Landeau B, Papathanassiou D, Crivello F, Etard O, Delcroix N, et al. Automated Anatomical Labeling of Activations in SPM Using a Macroscopic Anatomical Parcellation of the MNI MRI Single-Subject Brain. Neuroimage [Internet]. 2002 Jan 1 [cited 2019 Mar 13];15(1):273–89. Available from: https://www.sciencedirect.com/science/article/pii/S1053811901909784

44. Rubega M, Carboni M, Seeber M, Pascucci D, Tourbier S, Toscano G, et al. Estimating EEG Source Dipole Orientation Based on Singular-value Decomposition for Connectivity Analysis. Brain Topogr [Internet]. 2018 Dec 3 [cited 2019 Mar 13];1–16. Available from: http://link.springer.com/10.1007/s10548-018-0691-2

45. Rubega M., Pascucci D., Ru ́e Queralt J., Van Mierlo P., Hagmann P., Plomp G. MCM. Time-varying effective EEG source connectivity: The optimization of model parameters. In: 41st Annual International Conference of the IEEE Engineering in Medicine and Biology Society (EMBC), IEEE. 2019.

46. Milde T, Leistritz L, Astolfi L, Miltner WHR, Weiss T, Babiloni F, et al. A new Kalman filter approach for the estimation of high-dimensional time-variant multivariate AR models and its application in analysis of laser-evoked brain potentials. Neuroimage [Internet]. 2010 Apr 15 [cited 2019 Mar 13];50(3):960–9. Available from: https://www.sciencedirect.com/science/article/pii/S1053811909013998

47. Takahashi DY, Baccalá LA, Sameshima K. Information theoretic interpretation of frequency domain connectivity measures. Biol Cybern [Internet]. 2010 Dec 14 [cited 2019 Mar 13];103(6):463–9. Available from: http://link.springer.com/10.1007/s00422-010-0410-x

48. Sameshima K, Baccala LA, Baccala LA. Methods in Brain Connectivity Inference through Multivariate Time Series Analysis [Internet]. Baccalá L, editor. CRC Press; 2014 [cited 2019 Mar 13]. (Frontiers in Neuroengineering Series; vol. 20145078). Available from: https://www.taylorfrancis.com/books/9781439845738

49. [Online]. Available: http://www.brain-connectivity-toolbox.net.

50. Bullmore E, Sporns O. The economy of brain network organization. Nat Rev Neurosci [Internet]. 2012 May 13 [cited 2019 Apr 7];13(5):336–49. Available from: http://www.nature.com/articles/nrn3214

51. Latora V, Marchiori M. Efficient Behavior of Small-World Networks. Phys Rev Lett [Internet]. 2001 Oct 17 [cited 2019 Mar 13];87(19):198701. Available from: https://link.aps.org/doi/10.1103/PhysRevLett.87.198701

52. Watts, D. J., Strogatz SH. Collective dynamics of “small-world” networks. Nature. 1998;393(6684):440–2.

53. Fagiolo G. Clustering in complex directed networks. Phys Rev E [Internet]. 2007 Aug 16 [cited 2019 Mar 13];76(2):026107. Available from: https://link.aps.org/doi/10.1103/PhysRevE.76.026107

54. Babiloni F, Cincotti F, Babiloni C, Carducci F, Mattia D, Astolfi L, et al. Estimation of the cortical functional connectivity with the multimodal integration of high-resolution EEG and fMRI data by directed transfer function. Neuroimage [Internet]. 2005 Jan 1 [cited 2019 Mar 13];24(1):118–31. Available from: https://www.sciencedirect.com/science/article/pii/S1053811904005646

55. Pessoa L, Adolphs R. Emotion processing and the amygdala: from a “low road” to “many roads” of evaluating biological significance. Nat Rev Neurosci [Internet]. 2010 Nov 1 [cited 2019 Apr 2];11(11):773–82. Available from: http://www.nature.com/articles/nrn2920

56. Zheng J, Anderson KL, Leal SL, Shestyuk A, Gulsen G, Mnatsakanyan L, et al. Amygdala-hippocampal dynamics during salient information processing. Nat Commun [Internet]. 2017 Feb 8 [cited 2019 Apr 2];8:14413. Available from: http://www.nature.com/doifinder/10.1038/ncomms14413

57. Freese, Jennifer L.; Amaral DG. Neuroanatomy of the primate amygdala. - PsycNET [Internet]. P. J. Whalen & E. A. Phelps, editor. New York, NY, US: Guilford Press; 2009 [cited 2019 Apr 2]. The human amygdala (pp. 3-42). Available from: https://psycnet.apa.org/record/2009-02740-001

58. Kober H, Barrett LF, Joseph J, Bliss-Moreau E, Lindquist K, Wager TD. Functional grouping and cortical–subcortical interactions in emotion: A meta-analysis of neuroimaging studies. Neuroimage [Internet]. 2008 Aug [cited 2019 Apr 2];42(2):998–1031. Available from: https://linkinghub.elsevier.com/retrieve/pii/S1053811908002942

59. Thomas Yeo BT, Krienen FM, Sepulcre J, Sabuncu MR, Lashkari D, Hollinshead M, et al. The organization of the human cerebral cortex estimated by intrinsic functional connectivity. J Neurophysiol [Internet]. 2011 Sep [cited 2019 Apr 2];106(3):1125–65. Available from: http://www.physiology.org/doi/10.1152/jn.00338.2011

60. Price JL, Drevets WC. Neurocircuitry of Mood Disorders. Neuropsychopharmacology [Internet]. 2010 Jan 19 [cited 2019 Apr 2];35(1):192–216. Available from: http://www.nature.com/articles/npp2009104

61. Hamilton JP, Chen MC, Gotlib IH. Neural systems approaches to understanding major depressive disorder: An intrinsic functional organization perspective. Neurobiol Dis [Internet]. 2013 Apr [cited 2019 Apr 2];52:4–11. Available from: https://linkinghub.elsevier.com/retrieve/pii/S0969996112000393

62. Ramasubbu R, Konduru N, Cortese F, Bray S, Gaxiola-Valdez I, Goodyear B. Reduced Intrinsic Connectivity of Amygdala in Adults with Major Depressive Disorder. Front Psychiatry [Internet]. 2014 [cited 2019 Apr 2];5. Available from: http://journal.frontiersin.org/article/10.3389/fpsyt.2014.00017/abstract

63. Kaiser RH, Andrews-Hanna JR, Wager TD, Pizzagalli DA. Large-Scale Network Dysfunction in Major Depressive Disorder. JAMA Psychiatry [Internet]. 2015 Jun 1 [cited 2019 Apr 2];72(6):603. Available from: http://archpsyc.jamanetwork.com/article.aspx?doi=10.1001/jamapsychiatry.2015.0071

64. Tang S, Lu L, Zhang L, Hu X, Bu X, Li H, et al. Abnormal amygdala resting-state functional connectivity in adults and adolescents with major depressive disorder: A comparative meta-analysis. EBioMedicine [Internet]. 2018 Oct [cited 2019 Apr 2];36:436–45. Available from: https://linkinghub.elsevier.com/retrieve/pii/S2352396418303682

65. van Eijndhoven P, van Wingen G, van Oijen K, Rijpkema M, Goraj B, Jan Verkes R, et al. Amygdala Volume Marks the Acute State in the Early Course of Depression. Biol Psychiatry [Internet]. 2009 May [cited 2019 Apr 2];65(9):812–8. Available from: https://linkinghub.elsevier.com/retrieve/pii/S0006322308013140

66. Sandu A-L, Artiges E, Galinowski A, Gallarda T, Bellivier F, Lemaitre H, et al. Amygdala and regional volumes in treatment-resistant *versus* nontreatment-resistant depression patients. Depress Anxiety [Internet]. 2017 Nov [cited 2019 Apr 2];34(11):1065–71. Available from: http://doi.wiley.com/10.1002/da.22675

67. Bauer IE, Sanches M, Suchting R, Green CE, El Fangary NM, Zunta–Soares GB, et al. Amygdala enlargement in unaffected offspring of bipolar parents. J Psychiatr Res [Internet]. 2014 Dec [cited 2019 Apr 2];59:200–5. Available from: https://linkinghub.elsevier.com/retrieve/pii/S0022395614002660

68. Inman CS, Manns JR, Bijanki KR, Bass DI, Hamann S, Drane DL, et al. Direct electrical stimulation of the amygdala enhances declarative memory in humans. Proc Natl Acad Sci [Internet]. 2018 Jan 2 [cited 2019 Apr 3];115(1):98–103. Available from: http://www.pnas.org/lookup/doi/10.1073/pnas.1714058114

69. Bijanki KR, Kovach CK, McCormick LM, Kawasaki H, Dlouhy BJ, Feinstein J, et al. Case Report: Stimulation of the Right Amygdala Induces Transient Changes in Affective Bias. Brain Stimul [Internet]. 2014 Sep [cited 2019 Apr 2];7(5):690–3. Available from: https://linkinghub.elsevier.com/retrieve/pii/S1935861X14001752

70. Tyrand R, Seeck M, Pollo C, Boëx C. Effects of amygdala–hippocampal stimulation on synchronization. Epilepsy Res [Internet]. 2014 Feb [cited 2019 Apr 3];108(2):327–30. Available from: https://linkinghub.elsevier.com/retrieve/pii/S0920121113003215

71. Tyrand R, Seeck M, Spinelli L, Pralong E, Vulliémoz S, Foletti G, et al. Effects of amygdala–

hippocampal stimulation on interictal epileptic discharges. Epilepsy Res [Internet]. 2012 Mar [cited 2019 Apr 3];99(1–2):87–93. Available from: https://linkinghub.elsevier.com/retrieve/pii/S0920121111003342

72. Langevin J-P, Chen J, Koek R, Sultzer D, Mandelkern M, Schwartz H, et al. Deep Brain Stimulation of the Basolateral Amygdala: Targeting Technique and Electrodiagnostic Findings. Brain Sci [Internet]. 2016 Aug 10 [cited 2019 Apr 3];6(3):28. Available from: http://www.mdpi.com/2076-3425/6/3/28

73. Koek RJ, Langevin J-P, Krahl SE, Kosoyan HJ, Schwartz HN, Chen JW, et al. Deep brain stimulation of the basolateral amygdala for treatment-refractory combat post-traumatic stress disorder (PTSD): study protocol for a pilot randomized controlled trial with blinded, staggered onset of stimulation. Trials [Internet]. 2014 Dec 10 [cited 2019 Apr 3];15(1):356. Available from: https://trialsjournal.biomedcentral.com/articles/10.1186/1745-6215-15-356

74. Sturm V, Fricke O, Bührle CP, Lenartz D, Maarouf M, Treuer H, et al. DBS in the basolateral amygdala improves symptoms of autism and related self-injurious behavior: a case report and hypothesis on the pathogenesis of the disorder. Front Hum Neurosci [Internet]. 2013 [cited 2019 Apr 3];6:341. Available from: http://www.ncbi.nlm.nih.gov/pubmed/23346052

75. Marchand WR, Yurgelun-Todd D. Striatal structure and function in mood disorders: a comprehensive review. Bipolar Disord [Internet]. 2010 Dec [cited 2019 Apr 4];12(8):764–85. Available from: http://doi.wiley.com/10.1111/j.1399-5618.2010.00874.x

76. Bluhm R, Williamson P, Lanius R, ThÃ©berge J, Densmore M, Bartha R, et al. Resting state default-mode network connectivity in early depression using a seed region-of-interest analysis: Decreased connectivity with caudate nucleus. Psychiatry Clin Neurosci [Internet]. 2009 Dec [cited 2019 Apr 3];63(6):754–61. Available from: http://doi.wiley.com/10.1111/j.1440-1819.2009.02030.x

77. Butters MA, Aizenstein HJ, Hayashi KM, Meltzer CC, Seaman J, Reynolds CF, et al. Three-Dimensional Surface Mapping of the Caudate Nucleus in Late-Life Depression. Am J Geriatr Psychiatry [Internet]. 2009 Jan [cited 2019 Apr 3];17(1):4–12. Available from: https://linkinghub.elsevier.com/retrieve/pii/S1064748112607180

78. Ma C, Ding J, Li J, Guo W, Long Z, Liu F, et al. Resting-State Functional Connectivity Bias of Middle Temporal Gyrus and Caudate with Altered Gray Matter Volume in Major Depression. Fan Y, editor. PLoS One [Internet]. 2012 Sep 24 [cited 2019 Apr 3];7(9):e45263. Available from: http://dx.plos.org/10.1371/journal.pone.0045263

79. Krishnan KRR. Magnetic Resonance Imaging of the Caudate Nuclei in Depression. Arch Gen Psychiatry [Internet]. 1992 Jul 1 [cited 2019 Apr 3];49(7):553. Available from: http://archpsyc.jamanetwork.com/article.aspx?doi=10.1001/archpsyc.1992.01820070047007

80. Khundakar A, Morris C, Oakley A, Thomas AJ. Morphometric Analysis of Neuronal and Glial Cell Pathology in the Caudate Nucleus in Late-Life Depression. Am J Geriatr Psychiatry [Internet]. 2011 Feb [cited 2019 Apr 3];19(2):132–41. Available from: https://linkinghub.elsevier.com/retrieve/pii/S1064748112601584

81. Hannestad J, Taylor WD, McQuoid DR, Payne ME, Krishnan KRR, Steffens DC, et al. White

matter lesion volumes and caudate volumes in late-life depression. Int J Geriatr Psychiatry [Internet]. 2006 Dec [cited 2019 Apr 3];21(12):1193–8. Available from: http://doi.wiley.com/10.1002/gps.1640

82. Pillay S. A quantitative magnetic resonance imaging study of caudate and lenticular nucleus gray matter volume in primary unipolar major depression: relationship to treatment response and clinical severity. Psychiatry Res Neuroimaging [Internet]. 1998 Dec 14 [cited 2019 Apr 3];84(2–3):61–74. Available from: http://linkinghub.elsevier.com/retrieve/pii/S0925492798000481

83. Price JL, Drevets WC. Neural circuits underlying the pathophysiology of mood disorders. Trends Cogn Sci [Internet]. 2012 Jan [cited 2019 Apr 4];16(1):61–71. Available from: https://linkinghub.elsevier.com/retrieve/pii/S1364661311002622

84. Limbic-cortical dysregulation: a proposed model of depression. J Neuropsychiatry Clin Neurosci [Internet]. 1997 Aug [cited 2019 Apr 7];9(3):471–81. Available from: http://psychiatryonline.org/doi/abs/10.1176/jnp.9.3.471

85. Pizzagalli DA. Frontocingulate Dysfunction in Depression: Toward Biomarkers of Treatment Response. Neuropsychopharmacology [Internet]. 2011 Jan 22 [cited 2019 Apr 7];36(1):183–206. Available from: http://www.nature.com/articles/npp2010166

86. Seeber M, Cantonas L-M, Hoevels M, Sesia T, Visser-Vandewalle V, Michel CM. Subcortical electrophysiological activity is detectable with high-density EEG source imaging. Nat Commun [Internet]. 2019 Dec 14 [cited 2019 Mar 28];10(1):753. Available from: http://www.nature.com/articles/s41467-019-08725-w

87. Aouizerate B, Cuny E, Martin-Guehl C, Guehl D, Amieva H, Benazzouz A, et al. Deep brain stimulation of the ventral caudate nucleus in the treatment of obsessive—compulsive disorder and major depression. J Neurosurg [Internet]. 2004 Oct [cited 2019 Apr 3];101(4):682–6. Available from: https://thejns.org/view/journals/j-neurosurg/101/4/article-p682.xml

88. Millet B, Jaafari N, Polosan M, Baup N, Giordana B, Haegelen C, et al. Limbic versus cognitive target for deep brain stimulation in treatment-resistant depression: Accumbens more promising than caudate. Eur Neuropsychopharmacol [Internet]. 2014 Aug [cited 2019 Apr 3];24(8):1229–39. Available from: https://linkinghub.elsevier.com/retrieve/pii/S0924977X14001448

89. Grin-Yatsenko VA, Baas I, Ponomarev VA, Kropotov JD. EEG Power Spectra at Early Stages of Depressive Disorders. J Clin Neurophysiol [Internet]. 2009 Dec [cited 2019 Apr 4];26(6):401–6. Available from: https://insights.ovid.com/crossref?an=00004691-200912000-00003

90. Pollock VE, Schneider LS. Topographic Quantitative EEG in Elderly Subjects with Major Depression. Psychophysiology [Internet]. 1990 Jul [cited 2019 Apr 4];27(4):438–44. Available from: http://doi.wiley.com/10.1111/j.1469-8986.1990.tb02340.x

91. Roemer RA, Shagass C, Dubin W, Jaffe R, Siegal L. Quantitative EEG in elderly depressives. Brain Topogr [Internet]. 1992 [cited 2019 Apr 4];4(4):285–90. Available from: http://link.springer.com/10.1007/BF01135566

92. Kwon JS, Youn T, Jung HY. Right hemisphere abnormalities in major depression: Quantitative electroencephalographic findings before and after treatment. J Affect Disord [Internet]. 1996 Oct [cited 2019 Apr 4];40(3):169–73. Available from: http://linkinghub.elsevier.com/retrieve/pii/0165032796000572

93. Jiang H, Popov T, Jylänki P, Bi K, Yao Z, Lu Q, et al. Predictability of depression severity based on posterior alpha oscillations. Clin Neurophysiol [Internet]. 2016 Apr [cited 2019 Apr 4];127(4):2108–14. Available from: https://linkinghub.elsevier.com/retrieve/pii/S1388245716000031

94. Neumann W-J, Huebl J, Brücke C, Gabriëls L, Bajbouj M, Merkl A, et al. Different patterns of local field potentials from limbic DBS targets in patients with major depressive and obsessive compulsive disorder. Mol Psychiatry [Internet]. 2014 [cited 2019 Apr 5];19:1186–92. Available from: www.fil.ion.ucl.ac.uk/spm/

95. Bazire Stephen. Benzodiazepine equivalent doses. Psychotropic Drug Directory. Lloyd-Reinhold Communications; 2014.

14 Data Availability Statement

The raw data supporting the conclusions of this manuscript will be made available by the authors, without undue reservation, to any qualified researcher.